*Desalination and Water Treatment*
www.deswater.com

doi: 10.1080/19443994.2016.1172031

57 (2016) 29517–29530
December

Taylor & Francis
Taylor & Francis Group

# Comparative study of acid blue 113 wastewater degradation and mineralization by UV/persulfate and UV/Oxone processes

Hung-Yee Shu*, Shi-Wei Huang, Meng-Ke Tsai

*Institute of Environmental Engineering, Hungkuang University, Taichung 433, Taiwan, Tel. +886 426318652, ext. 1200; email: hyshu@sunrise.hk.edu.tw (H.-Y. Shu), Tel. +886 426318652, ext. 4123; emails: love85262@yahoo.com.tw (S.-W. Huang), mysterykissu@gmail.com (M.-K. Tsai)*

Received 10 January 2016; Accepted 24 March 2016

ABSTRACT

Sulfate radical-based advanced oxidation processes (SR-AOPs) are powerful technologies to treat various pollutants. Among these SR-AOPs, UV/persulfate (UV/PS) and UV/Oxone were chosen to degrade and mineralize Acid Blue 113 (AB113) wastewater for their strong reactivity. The experimental setup was designed identical to compare two processes. Operating parameters such as oxidant dosage, UV intensity, initial dye concentration, and pH were studied to evaluate their effects on degradation and mineralization of AB113. The results demonstrated powerful degradation of AB113 and mineralization rate for both UV/PS and UV/Oxone processes. However, reaction with either UV irradiation alone or persulfate alone can reach low removal efficiency of AB113. But Oxone oxidation alone can achieve about 95% of AB113 removal efficiency. For both UV/PS and UV/Oxone processes, the higher the oxidant dosage applied, the higher the AB113 and TOC removal efficiencies can be obtained up to the optimal dosage. On the other hand, the AB113 removal efficiency and reaction rate constant decreased with increasing in the initial AB113 concentration. The initial pH showed no significant effect on AB113 removal efficiency. UV/Oxone process was observed to be more sensitive to UV intensity and pH on TOC mineralization. The lower UV power conducted lower TOC mineralization.

*Keywords:* Azo dye; Degradation; Mineralization; Oxone; Peroxymonosulfate; Persulfate; Sulfate radical; UV

## 1. Introduction

Effluent containing dyestuffs from textile industry often draws attention of the government, public, and scientific research communities. In general, process water from dyeing operation contains residual dyestuff in certain amount which will be discharged to a traditional treatment facility equipped with coagulation and activated sludge processes. Unfortunately, coagulation process can only remove color caused by dyestuff poorly, and causes sludge treatment problem [1]. Activated sludge process is constrained by dyestuff toxicity and complication compositions to be properly operated [2]. In order to meet stringent color

---

*Corresponding author.

*Presented at the 8th International Conference on Challenges in Environmental Science & Engineering (CESE-2015)*
*28 September–2 October 2015, Sydney, Australia*

1944-3994/1944-3986

discharge standard, perchlorate is usually employed to decolorize dye containing wastewater. However, this approach causes serious environmental concern with formation of carcinogenic chlorinated organic compounds [1]. Therefore, more efficient technologies with low environmental impact should be developed to dealing with complicated dyeing wastewater. The target pollutant, Acid Blue 113, of this work belongs to the azo dye group. Azo dyes with nitrogen double bond (–N=N–) are the largest class of commercial dyestuffs used in the textile industries. Among literature review outcomes, many researchers have reported their investigations on various technologies for degradation of azo dye wastewaters [3–7].

Traditionally, a group of technologies called advanced oxidation processes (AOPs) which employ alternative combinations of UV irradiation, oxidants such as ozone, hydrogen peroxide and Fenton reagents, and photo-catalysts ($TiO_2$ and ZnO) to produce hydroxyl radicals (HR) for non-selectively degradation of recalcitrant organic compounds [8]. All of the hydroxyl radical-based advanced oxidation processes (HR-AOPs) utilize HR which is the most powerful oxidant for pollutant treatment. Therefore, HR-AOPs are able to mineralize pollutants in to the simplest final products of carbon dioxide and water. Wide range of environmental pollutants can be thoroughly degraded by HR-AOPs. For target pollutant, azo dye wastewater, HR-AOPs including $UV/H_2O_2$ [9,10], $UV/O_3$ [7], and Fenton reaction [11] as well as photo catalyst application i.e. $UV/TiO_2$ and UV/ZnO [2,12], have been reported to degrade and mineralize azo dye wastewater successfully.

In the last decade, AOPs employing sulfate radicals, $SO_4^{-\bullet}$, (SR-AOPs) as alternative AOPs to the traditional HR-AOPs have attracted a great attention on wastewater treatment applications. In general, SR-AOPs utilize either persulfate (PS) or peroxymonosulfate (PMS) as oxidant to be further activated for producing sulfate radicals. Originally, PS was used for *in situ* chemical oxidation (ISCO) technology to remedy groundwater and soil contaminants with its merit of stability [13]. Differently, PMS was an important oxidant for organic synthesis process for various organic chemicals such as epoxide [14], selenones [15], and dithiirane derivatives [16], etc. Both PS and PMS can be transformed into sulfate radicals through heat [17,18], UV irradiation [19,20], and chemically activated with transition metal ions [21–23] which results powerful sulfate radicals with high oxidation–reduction potential (ORP) of +2.5 to +3.1 V [23] to degrade refractory pollutants in wastewater. Persulfate anion can be activated by UV irradiation to form sulfate radicals ($SO_4^{-\bullet}$) as presented by follows:

$$S_2O_8^{2-} \xrightarrow{hv} 2SO_4^{-\bullet} \tag{1}$$

Similarly, peroxymonosulfate anion can be activated by UV irradiation to form sulfate radicals and HR as presented by follows:

$$HSO_5^- \xrightarrow{hv} OH^{\bullet} + SO_4^{-\bullet} \tag{2}$$

The above-mentioned reaction equations support the fundamentals of SR-AOPs, i.e. UV/persulfate (UV/PS) and UV/peroxymonosulfate (UV/PMS) processes. The advantage of sulfate radical is its stability in comparison with hydroxyl radical in aqueous [24]. PS is a strong oxidant with 2.01 V of high ORP as well as PMS. However, it shows less reactive to the pollutants at ambient condition [25]. To overcome this disadvantage, PS (or PMS) activated by UV irradiation can produce sulfate radicals with even higher ORP [23,26,27].

Previously, SR-AOPs have been gaining involvement to the environmental applications [28] which includes the treatment of dye wastewater [29], chlorophenols [19,30], landfill leachate [31], personal care pharmaceuticals [32], and pesticides [33]. Some literatures compare the capability of UV/PS and $UV/H_2O_2$ processes for their treatment performances of polyvinyl alcohol, atrazine cylindrospermopsin, and bisphenol A. Based on the pseudo-first-order rate constant and removal efficiency, in most of the cases, UV/PS demonstrates more powerful to degrade pollutants than $UV/H_2O_2$ process [34–37]. In contrast, Tan et al. concludes a case that $UV/H_2O_2$ performed better degradation capability on treatment of antipyrine [38]. Furthermore, on very concerned toxicity issue, the *V. fisheri* toxicity of bisphenol A is fast declined to non-toxic level in 10 min of reaction time by UV/PS process. On the other hand, the *V. fisheri* toxicity of bisphenol A increases to the highest toxicity in 30 min reaction time, then gradually decreases to non-toxic level to the end of reaction by $UV/H_2O_2$ process [39]. This also demonstrates the beneficial effect of UV/PS process.

The aim of this work is to compare two SR-AOPs i.e. UV/PS and UV/Oxone processes on the treatment capabilities of C.I. Acid Blue 113 (AB113) wastewater samples. Both of the AOPs utilize an identical recirculated thin gap annular photochemical reactor in which the UV 254 irradiation on persulfate (or Oxone) to produce sulfate radicals was conducted. The effects of various operating parameters such as oxidant dosage, UV intensity, initial dye concentration, and initial pH on degradation and mineralization of AB113 were investigated for both SR-AOPs. Changes in AB113 concentration, total organic carbon (TOC), pH, oxidation reduction potential (ORP) were monitored to evaluate the performance of these two SR-AOPs.

## 2. Materials and methods

### 2.1. Materials and apparatus

Reagent grade Sodium Persulfate ($Na_2S_2O_8$) with 550 g $L^{-1}$ solubility and commercially available peroxymonosulfate, with trade name Oxone ($KHSO_4 \cdot K_2SO_4 \cdot KHSO_5$, containing 42% of $KHSO_5$), were purchased from Merck, Inc. A dis-azo dye, C.I. Acid Blue 113 (AB113) with molecular weight of 681.66 g $mol^{-1}$, 50% purity was purchased from Sigma–Aldrich, Inc. and used as received without further purification. The chemical properties of AB113 can be obtained from our previous study [40].

The AB113 degradation and mineralization by UV/PS and UV/Oxone processes experiments were conducted in an identical experimental setup scheme as shown in Fig. 1 to compare the capabilities of two SR-AOPs. From the Figure, a thin gap photochemical reactor is equipped with a one liter stirring tank reactor to recirculate and photochemical treatment of AB113 wastewater. The photochemical reactor is confined with a stainless steel outer shell (ID = 2.8 cm, $L$ = 85 cm). Alone the stainless shell, an input tubing position is located at bottom and an output tubing position is located at the top as well. At the center of photochemical reactor, a quartz pipe with outer diameter of 2.0 cm and length of 85 cm is fixed to protect the UV lamp. Inside the quartz pipe, a Phillip made low pressure mercury UV lamp with irradiation wavelength 253.7 nm and input power of 30 watts is employed. The UV light intensity of 30 W yielded a surface light energy of 5.6 mW $cm^{-2}$ measured at the outer surface of quartz tube. During the experiments of UV/PS and UV/Oxone processes, the one liter wastewater with designated AB113 concentration and oxidant dosage was prepared in the one-liter stirring tank reactor and continuously monitored with pH and ORP probes. At the beginning of the experiment, wastewater was pumped through the input port of photochemical reactor and discharged through the output port, then flowed back to the stirring tank reactor for recirculation purpose. Once the UV lamp is turned on, the timer started to keep right sampling time intervals. Then, samples were analyzed by UV–vis spectrophotometer and TOC analyzer.

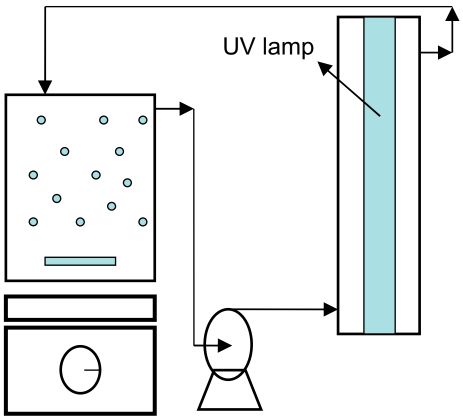

Fig. 1. The schematic drawing of the thin gap annular photochemical reactor employed.

### 2.2. Experimental procedure and analysis

The operating parameters studied included reaction time, oxidant (persulfate or Oxone) dosage, UV intensity, initial AB113 concentration, and initial pH value. AB113 wastewater samples at various AB113 concentrations (50–400 mg $L^{-1}$) and oxidant dosages (0.21–6.3 mM) were prepared with deionized water and various amounts of AB113 and oxidant. In the case of pH effect study, the experiments were conducted by adjusting the initial pH value of 5.8 to the range of 2–10 using HCl and/or NaOH with initial AB113 concentration of 50 mg $L^{-1}$ and persulfate (or Oxone) dosage 6.3 mM. It is to reflect the real wastewater treatment plant operation and dyebath operation as well, HCl and NaOH were used to adjust pH value to a suitable condition for operation, although, the chloride ion may contribute the AOP process as a free radical scavenger. Similarly, for UV intensity study, the UV lamp was connected to a voltage regulator to adjust the UV lamp surface intensities to 2.0–5.6 mW $cm^{-2}$. In order to represent the UV power conducted to the UV/PS or UV/Oxone process, the UV input energy was divided by treatment volume as a volumetric specific UV intensity in W $L^{-1}$, and used in this work.

At a predetermined reaction time, an aliquot of the solution was withdrawn and analyzed for residual AB113 concentration, TOC, and color intensity. AB113 concentration was determined by measuring the absorbance at characterized wavelength of 566 nm using Hitachi U-2000 spectrophotometer. Color intensity measurement followed the American Dye Manufacturers Institute (ADMI) standard color measurement by applying the Adams-Nickerson color difference formula referencing to method 2120E of the Standard Methods. The pH and redox potential (ORP) were monitored by a Eutech PH5500 dual channel pH/ion meter with specific probes. TOC was obtained with a total organic carbon analyzer from O.I. Analytical Aurora, model 1030.

## 3. Results and discussion

### 3.1. Control experiments

The oxidative degradation and mineralization of target pollutant, AB113, were demonstrated by comparing three single approaches (UV irradiation, persulfate oxidation, and Oxone oxidation) and integrated processes i.e. UV/PS and UV/Oxone technologies. The operating parameters were set at the initial AB113 concentration of 50 mg $L^{-1}$, Oxidant (sodium persulfate or Oxone) dosage of 4.2 mM, and UV light intensity of 30 W $L^{-1}$ at wavelength of 254 nm in 120 min of reaction. Fig. 2(a) presents the results of AB113 removal by UV irradiation, persulfate oxidation, and Oxone oxidation approaches. The removal curves show that UV irradiation can degrade AB113 to 66.0% in 120 min irradiation time. This demonstrates that AB113 dye molecule can be photo degraded to moderate level to break its chromophore bonding. The observation implies that under UV irradiation, the dye molecule is excited by UV energy to form unstable intermediates and resulting to breaking of chromophore after the UV excitation. However, the UV irradiation is not able to further mineralize the organic carbons on the dye molecules. Therefore, barely change on TOC is observed. Persulfate and Oxone are both very strong oxidants which are able to oxidative degrade pollutants in wastewater. By adding 4.2 mM sodium persulfate into the AB113 wastewater, AB113 was exponentially removed up to 44.6% in 120 min oxidation time. As for the case of Oxone oxidative degradation of AB113, Oxone process alone was more effective than that of persulfate process. The process achieved 95.1% AB113 removal efficiency. On the other hand, no observable TOC mineralization was measured for both persulfate and Oxone oxidation processes.

The SR-AOP integrates UV irradiation and persulfate oxidant (or Oxone) can produce sulfate radical which is the stronger oxidant to destruct pollutants than persulfate and Oxone. From Fig. 2(b), UV/PS and UV/Oxone perform almost same ability to degrade AB113. The results show that about 90 and 100% of AB113 removal efficiencies are reached in only 6 and 30 min for both SR-AOPs, respectively. Different from the UV irradiation and oxidant oxidation processes alone, the TOC mineralization efficiencies of AB113 under UV/PS and UV/Oxone processes are more thorough. TOC removal efficiencies reach 98.1 and 82.5% for UV/PS and UV/Oxone processes in 120 min, respectively. This demonstrates that both UV/PS and UV/Oxone processes are very powerful processes for AB113 degradation and mineralization.

The TOC value presents the TOC concentration in the solution. It is an important indicator of mineralization. At beginning of the sulfate radical oxidation reaction, solution TOC cannot be destroyed easily. At time region less than 20 min, large molecules were degraded to lower molecule weight intermediates which still contributed to TOC measurement. Therefore, at this region, TOC removal efficiency may remain almost unchanged. After this lag phase (20 min), TOC can be removed proportionally to the reaction time significantly. Therefore, the TOC removal efficiency increased from 7.0 and 7.5% at 20 min to 98.1 and 82.5% at 120 min, respectively. The original TOC of 50 mg $L^{-1}$ AB113 solution is 20.3 ± 0.5 mg $L^{-1}$ for both processes.

The pH values were monitored continuously during the reaction. The measurements presented that the pH changed toward acidic conditions as UV/PS and UV/Oxone oxidation occurring as shown in Fig. 2(c) and (d) for UV/PS and UV/Oxone processes, respectively. The pH value of UV/PS process changed significantly from initially pH 5.8–2.3 at the end of the degradation reaction. Similarly, the pH value changed shapely from initially pH 5.8–2.6 for UV/Oxone process. The observation is due to the production of organic acid byproducts and inorganic ions such as sulfate, chloride, nitrate, and nitrite ions under sulfate radical oxidation. Similar pH changes were observed in our previous AOP studies [2,12].

Another parameter monitored continuously during the reaction was ORP. ORP value can be used as a measure of the oxidizing or reduction power of the solution. In general, a higher positive solution ORP value represents an oxidizing environment which implies the presence of oxidizing reagents. In contrast, a lower negative ORP value represents a more reducing environment [41]. In this set of experiments, as shown in Fig. 2(c) and (d), the highest ORPs can be reached up to 544 and 754 mV for UV/PS and UV/Oxone processes, respectively. For persulfate oxidation process, the highest ORP value was 395 mV. On the other hand, the ORP was relatively unchanged at value of about 420 mV under UV irradiation alone, because no oxidant was added and no free radicals were formed. This observation explains UV/PS and UV/Oxone processes perform more powerful oxidative degradation than persulfate alone and UV irradiation alone processes due to the formation of sulfate radicals.

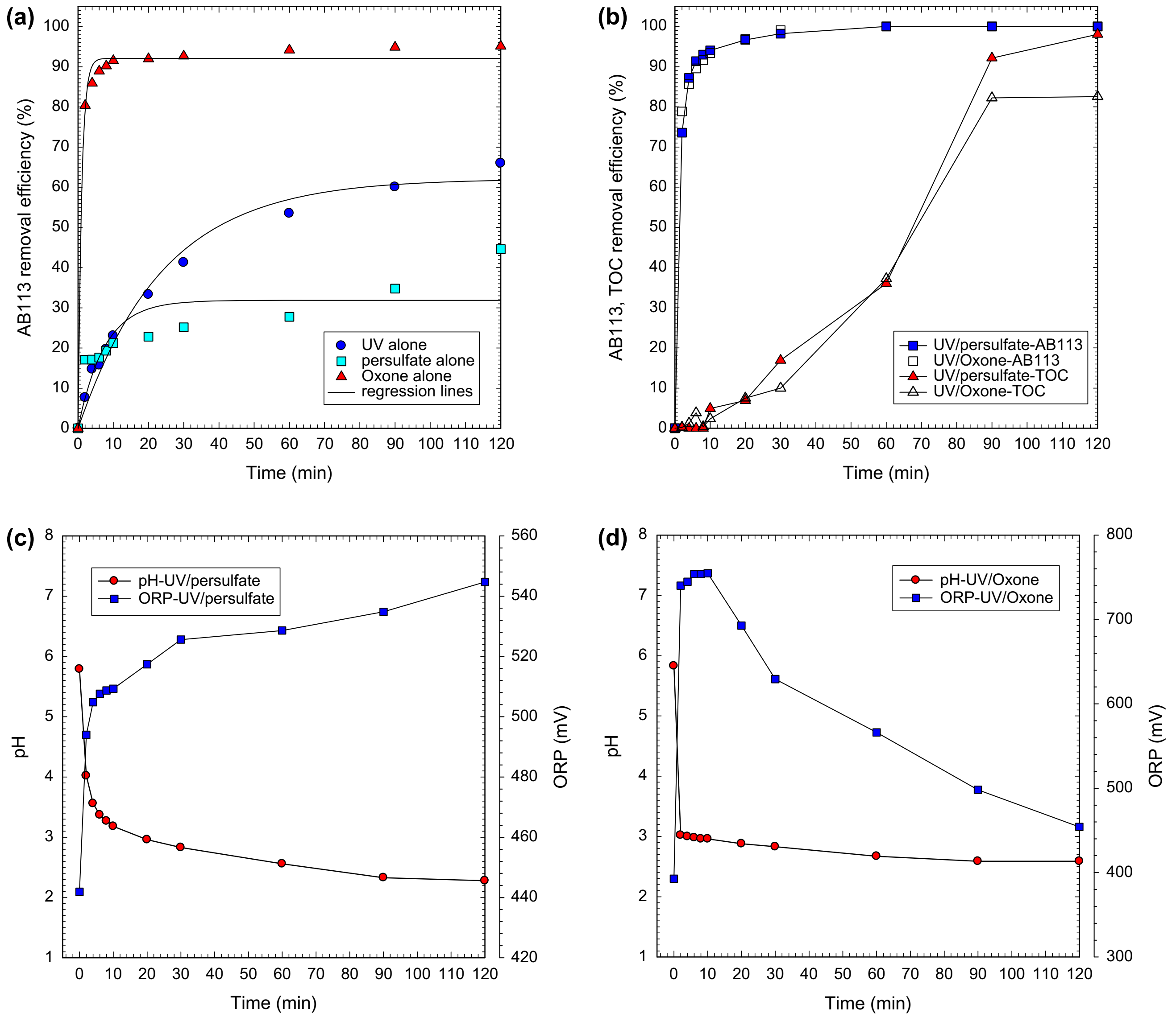

Fig. 2. (a) The comparisons of UV irradiation alone, persulfate oxidation alone, and Oxone alone processes on AB113 removal efficiency, (b) the comparisons of UV/PS and UV/Oxone processes on AB113 and TOC removal. The pH and ORP values during (c) UV/PS, and (d) UV/Oxone processes. The conditions were initial dye concentration of 50 mg $L^{-1}$, sodium persulfate (or Oxone) dosage 4.2 mM, UV dosage 30 W $L^{-1}$, (5.6 mW $cm^{-2}$), and reaction time during 120 min.

### 3.2. Proposed reaction kinetics

In most of the AOPs studies, the reaction kinetics is proposed to follow pseudo-first-order reaction. Therefore, the initial stage of AB113 degradation reaction under UV/PS and UV/Oxone processes can be described as follows.

$$C_{\mathrm{AB113}} = C_{\mathrm{AB113,0}} \times e^{-k_1 t} \qquad (3)$$

where $k_1$ denotes the pseudo-first-order reaction rate constant ($\mathrm{min}^{-1}$), $t$ is the reaction time (min), $C_{\mathrm{AB113,0}}$ designates the initial concentration (mg $L^{-1}$) of AB113, and $C_{\mathrm{AB113}}$ is the concentration (mg $L^{-1}$) of AB113 at time $t$. In order to calculate rate constant, $k_1$, Eq. (3) can be further transformed as follows.

$$-\ln\left(\frac{C_{\mathrm{AB113}}}{C_{\mathrm{AB113,0}}}\right) = k_1 \times t \qquad (4)$$

The curve fitting of experimental results by Eq. (4) can be used to obtain first-order rate constants. The rate constants followed similar trend as AB113 removal efficiency, the observed pseudo-first-order rate constants for UV/PS process were 0.1417 and 0.1112 $\text{min}^{-1}$ at AB113 initial concentration of 50 and 100 mg $\text{L}^{-1}$, respectively. Similarly, the pseudo-first-order rate constants for UV/Oxone process were 0.1276 and 0.0933 $\text{min}^{-1}$ at AB113 initial concentration of 50 and 100 mg $\text{L}^{-1}$, respectively. However, the regressions were with poor agreement ($r^2 = 0.642$–0.709). The results agree with other work, where the first-order rate constants were in the same range of 0.0908 $\text{min}^{-1}$ for Cibacron Brilliant Yellow 3 dye reported by Yeber et al. [30].

From our previous study, the experimental results from UV/Oxone process were found to follow pseudo-second-order reaction [42] and can be described as follows:

$$\frac{1}{C_{\text{AB113}}} - \frac{1}{C_{\text{AB113,0}}} = k_2 \times t \qquad (5)$$

where $k_2$ denotes the pseudo-second-order reaction rate constant ($\text{L mg}^{-1}\,\text{min}^{-1}$), $t$ is the reaction time (min), $C_{\text{AB113,0}}$ designates the initial concentration (mg $\text{L}^{-1}$) of AB113, and $C_{\text{AB113}}$ is the concentration (mg $\text{L}^{-1}$) of AB113 at time $t$.

Fig. 3 demonstrates the treatment of AB113 concentration change and curve fitting for the pseudo-second-order and pseudo-first-order rate expression using $1/C$ and $-\ln(C/C_0)$ vs. time curves. In Fig. 3(a), the curve fitting for pseudo-second-order presents very good fitting for both UV/PS and UV/Oxone processes at 50 and 100 mg $\text{L}^{-1}$ initial AB113 concentration. It implies that the reaction kinetics is very consistent with second-order kinetics ($r^2 = 0.903$–0.997). On the other hand, from Fig. 3(b), because the AB113 concentration drops sharply at first 2 min, thus, pseudo-first-order curve fitting shows two segments of linear lines before and after 2 min time. It makes the AB113 degradation data not agree well with pseudo-first-order kinetics ($r^2 = 0.642$–0.709). In most of AOPs study, the reaction kinetics can be simplified as pseudo-first-order. However, in this study, it is not suitable to assume first-order.

### 3.3. Effect of oxidant dosage

From our previous UV/$H_2O_2$ HR-AOP work, it was observed that when applied higher hydrogen peroxide dosage, the better pollutant removal efficiency can be reached [9]. The more HR is formed with higher hydrogen peroxide dosage applied under UV irradiation. Similar mechanisms can be conducted for SR-AOPs such as UV/PS and UV/Oxone processes.

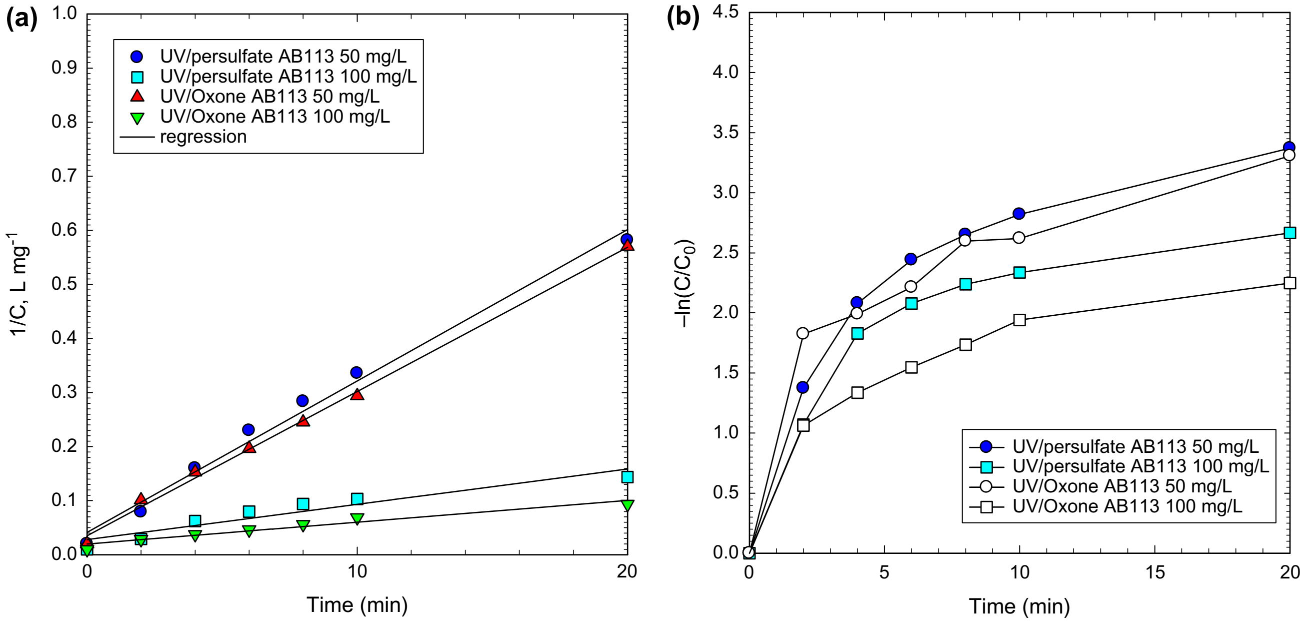

Fig. 3. (a) The pseudo-second-order kinetics curves and (b) pseudo-first-order kinetics curves for UV/PS, and UV/Oxone processes on AB113 concentration changes. The conditions were initial dye concentration of 50–100 mg $\text{L}^{-1}$, sodium persulfate (or Oxone) dosage 4.2 mM, UV dosage 30 W $\text{L}^{-1}$, (5.6 mW $\text{cm}^{-2}$), and reaction time during 20 min.

However, overdose of the hydrogen peroxide dosage to excess the optimal dosage may cause decline of the reaction rate and removal efficiency of pollutant. Because, the excess amount of hydrogen peroxide will compete with pollutant for free radicals to reduce the reaction rate and removal efficiency. To observe the oxidant dosage effect on removal of AB113 by proposed SR-AOPs, i.e. UV/PS and UV/Oxone, a set of experiments were performed. The effect of oxidant dosage on the degradation of AB113 was studied at initial AB113 concentrations of 50 mg $L^{-1}$, oxidant dosage of 0.21–6.3 mM, and 30 W $L^{-1}$ UV light intensity for a period of 120 min. Fig. 4(a) shows the degradation of AB113 as a function of persulfate dosage. Results present that the AB113 removal efficiency increases from 84.4 to 96.6% in 30 min when the persulfate dosage increases from 0.21 to 6.3 mM, respectively. This concludes that at higher persulfate dosage, higher AB113 removal efficiency is reached. From the figure, it also presents that at persulfate dosage higher than 2.1 mM, the degradation abilities for UV/PS process are almost the same. The results suggest that the higher persulfate dosage under UV irradiation can produce more sulfate radicals which contribute to the degradation of AB113 molecules. Therefore, the removal efficiency and degradation rate

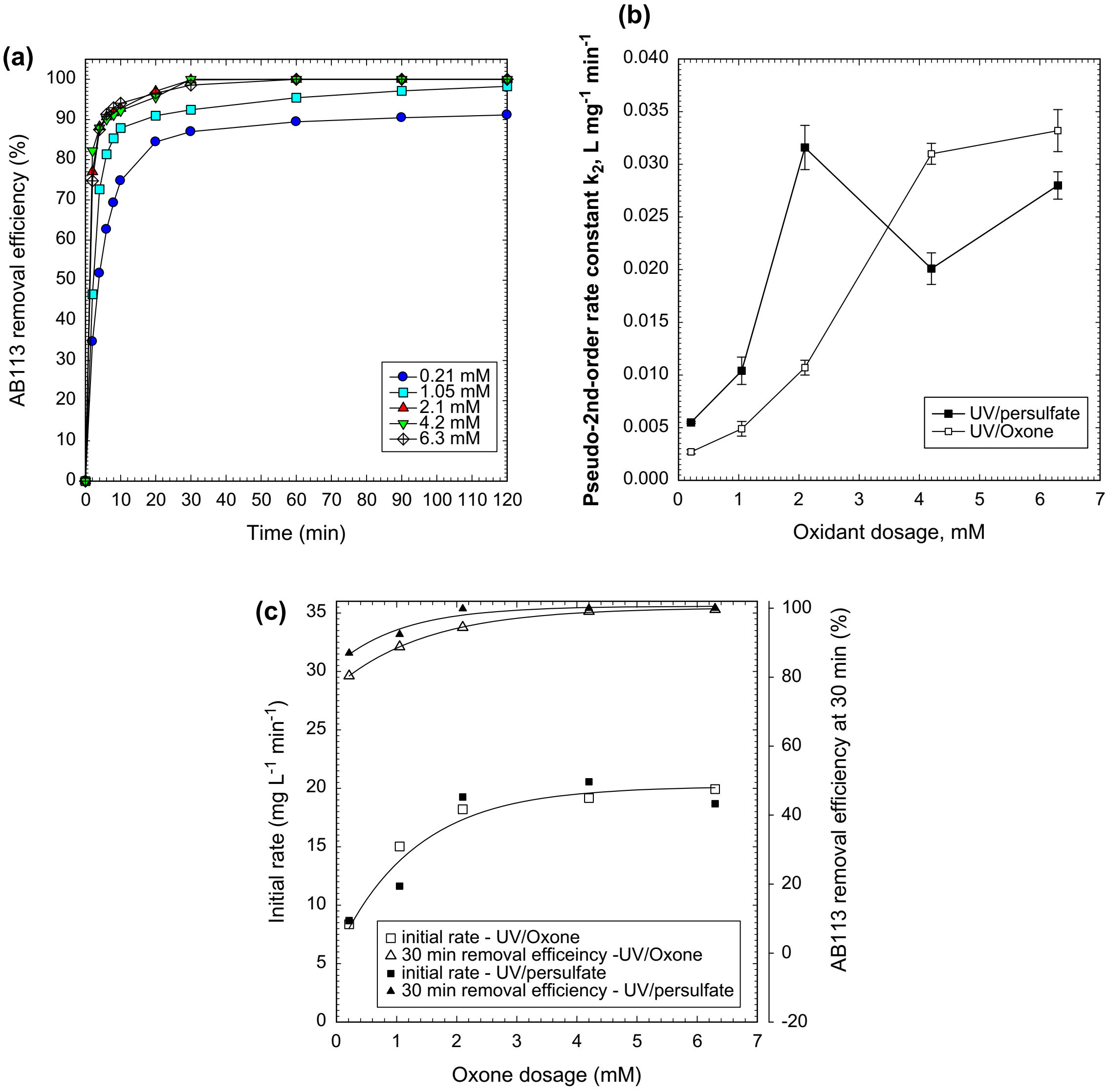

Fig. 4. Effect of oxidant dosage on (a) AB113 removal, (b) pseudo-second-order rate constant, and (c) initial rate and 30 min removal efficiency by UV/PS and UV/Oxone processes. The conditions were initial dye concentration of 50 mg $L^{-1}$, oxidant dosage 0.21–6.3 mM, UV light intensity of 30 W $L^{-1}$, (5.6 mW $cm^{-2}$) and reaction time during 120 min.

increases. As the persulfate dosage over 2.1 mM, the excess amount of persulfate reacts with sulfate radicals to form less reactive species such as persulfate ions. This mechanism conducts the decease of the reaction rate for dosage higher than optimal dosage. Similar observation was obtained by Kamel et al. for Congo red dye at 1.0–2.0 mM persulfate dosage [43]. Similar AB113 degradation behavior can be observed for UV/Oxone process, only the optimal dosage of Oxone was at 4.2 mM of Oxone. By applying pseudo-second-order reaction kinetics, the second-order rate constants can be obtained and summarized in Fig. 4(b). The results show that second-order rate constant increases almost proportionally till optimal dosage. After this optimal dosage, the second-order rate constant remains unchanged or declining.

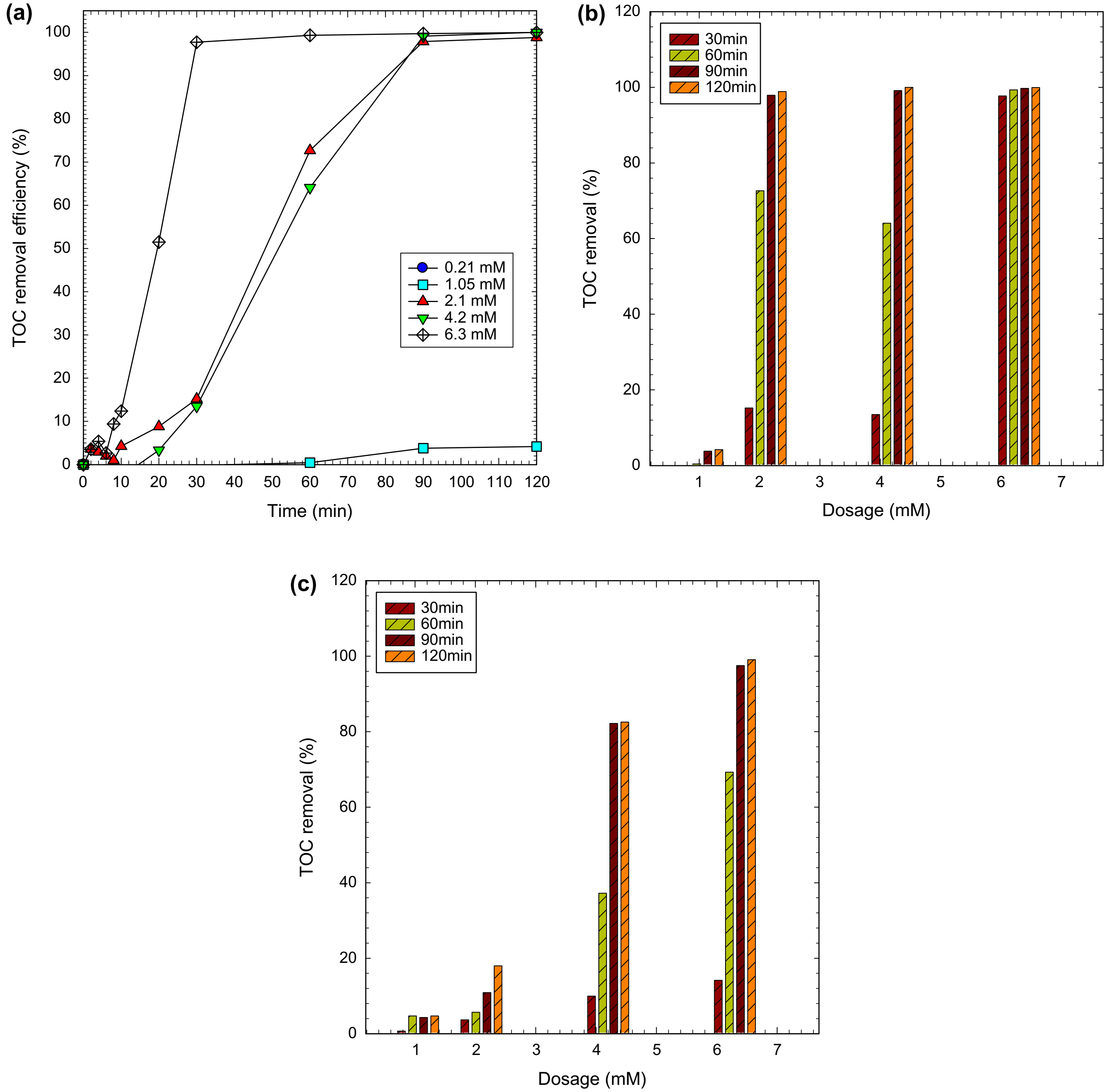

Fig. 5. Effect of oxidant dosage on TOC removal by (a) UV/PS, (b) UV/PS (bar chart), and (c) UV/Oxone (bar chart) processes. The conditions were the same as Fig. 4.

For oxidant dosage less than 2.1 mM, the UV/PS process has higher second-order rate constants than that of UV/Oxone process. For oxidant dosage higher than 2.1 mM, the rate constant for UV/Oxone process keeps increasing to reach same level as UV/PS process. As shown in Fig. 4(c), initial rate (mg $L^{-1}$ $min^{-1}$) for first 2 min of reaction and 30 min removal efficiency are presented for both UV/PS and UV/Oxone processes based on various oxidant dosages. From the figure, two processes show evenly powerful for degrading AB113 in wastewater.

As mentioned prior to this section, TOC removal efficiency presents a lag phase. Therefore, through 120 min reaction time, one can observe the effect of

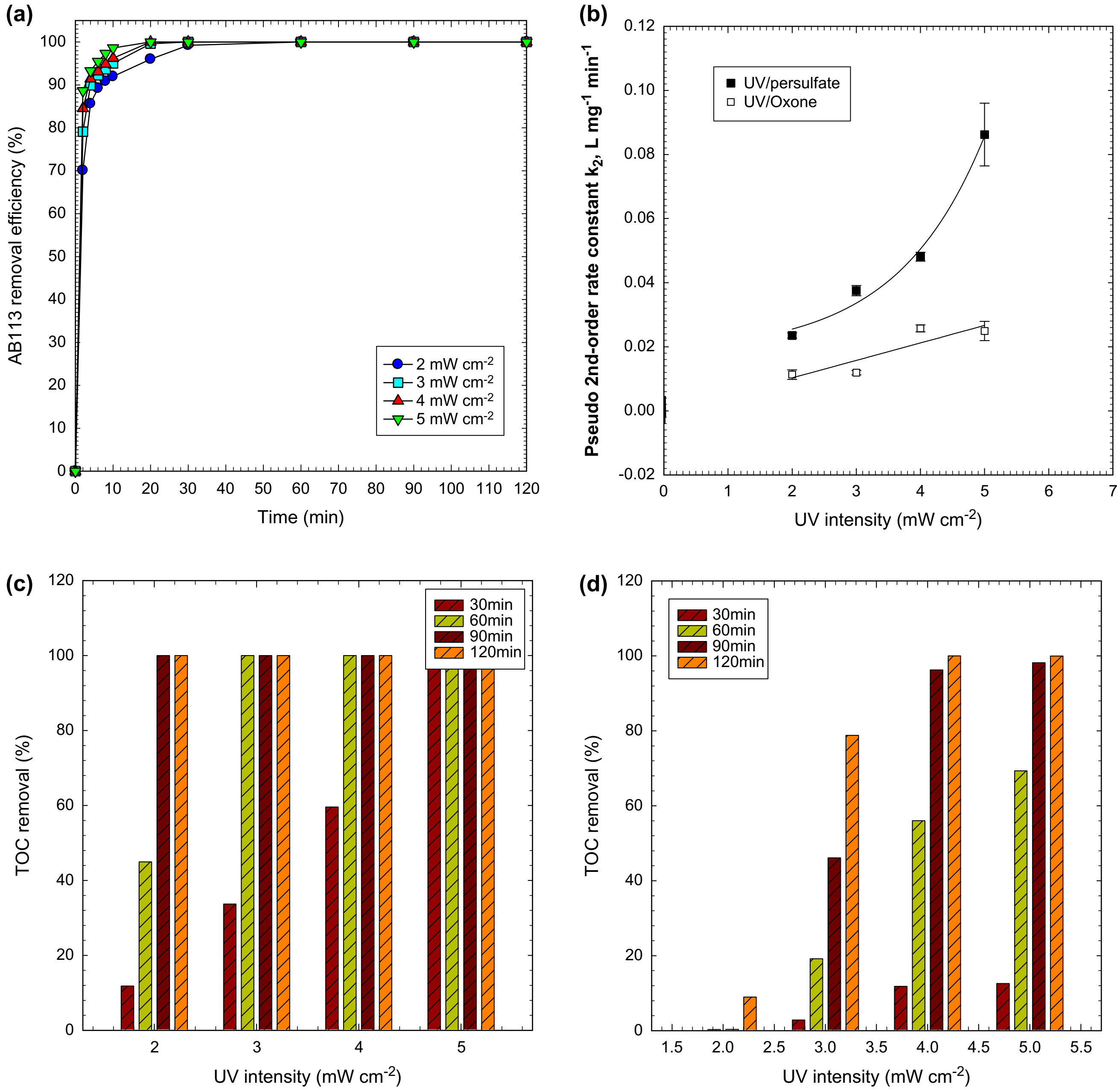

Fig. 6. Effect of UV intensity on (a) AB113 removal by UV/PS process, (b) second-order rate constant for UV/PS and UV/Oxone (c) TOC removal by UV/PS process, and (d) TOC removal by UV/Oxone process. The conditions were initial dye concentration of 50 mg $L^{-1}$, persulfate/Oxone dosage of 6.3 mM, UV light intensity 2–5 mW $cm^{-2}$ and reaction time during 120 min.

persulfate dosage on TOC removal efficiency under UV/PS process as shown in Fig. 5(a). In the figure, under low persulfate dosage as 0.21–1.05 mM, the TOC removal efficiency is nonsignificant. For higher persulfate dosage from 2.1 to 6.3 mM, TOC removal efficiencies increase proportionally up to 99% once pass the lag phase. To compare the TOC mineralization capabilities of UV/PS and UV/Oxone process, TOC removal efficiencies of 30–120 min for UV/PS and UV/Oxone processes are demonstrated as bar charts as Fig. 5(b) and (c), respectively. From the figures, TOC removal efficiencies can be reached to 99% for persulfate dosage higher than 2.1 mM and reaction time longer than 90 min under UV/PS process as shown in Fig. 5(b). The UV/Oxone process shows weaker capability for mineralizing AB113 TOC. For Oxone dosage of 4.2 and 6.3 mM, UV/Oxone process can only mineralize TOC to 82.2 and 97.5% at 90 min in comparison with UV/PS process, respectively. Results in Figs. 4 and 5 indicate that the TOC removal was more sensitive than AB113 removal on oxidant dosage. To simultaneously degrade AB113 and mineralize TOC, one should choose higher persulfate dosage to fulfil both AB113 dye and TOC removal requirements. At the meantime, TOC mineralization performance of the UV/Oxone process is more sensitive and limited by oxidant dosage than that of UV/PS process.

### 3.4. Effect of UV light intensity

UV intensity plays an important role on enhancing the treatment capability of pollutants by UV-based AOPs. For example, in UV/PS process, while applying the higher UV light intensity, the faster sulfate radical formation can be obtained. This results to the faster pollutant degradation and mineralization. Therefore, the rate constant increases by UV intensity increasing, while the same persulfate dosage applied. Because of high power UV irradiation on persulfate, abundant sulfate radicals are produced to react with target pollutants. It is obvious that the more UV intensity employed to the UV/PS process to degrade AB113, the faster the AB113 degradation and mineralization. Fig. 6 shows the removal of AB113 by UV/PS process as a function of UV intensity for 6.3 mM persulfate dosage. Results indicate that for highest persulfate dosage of 6.3 mM, the AB113 removal efficiencies were very close during whole reaction period. However, small differences between various UV intensities can be observed at beginning stage of the reaction which is the higher UV intensity resulting faster AB113 degradation. The removal efficiencies of AB113 by UV/Oxone process for various UV intensities demonstrate similar trends as UV/PS process (data not shown). To compare these two SR-AOPs, the effect of UV intensity on second-order rate constant is summarized in Fig. 6(b). From the figure, the second-order

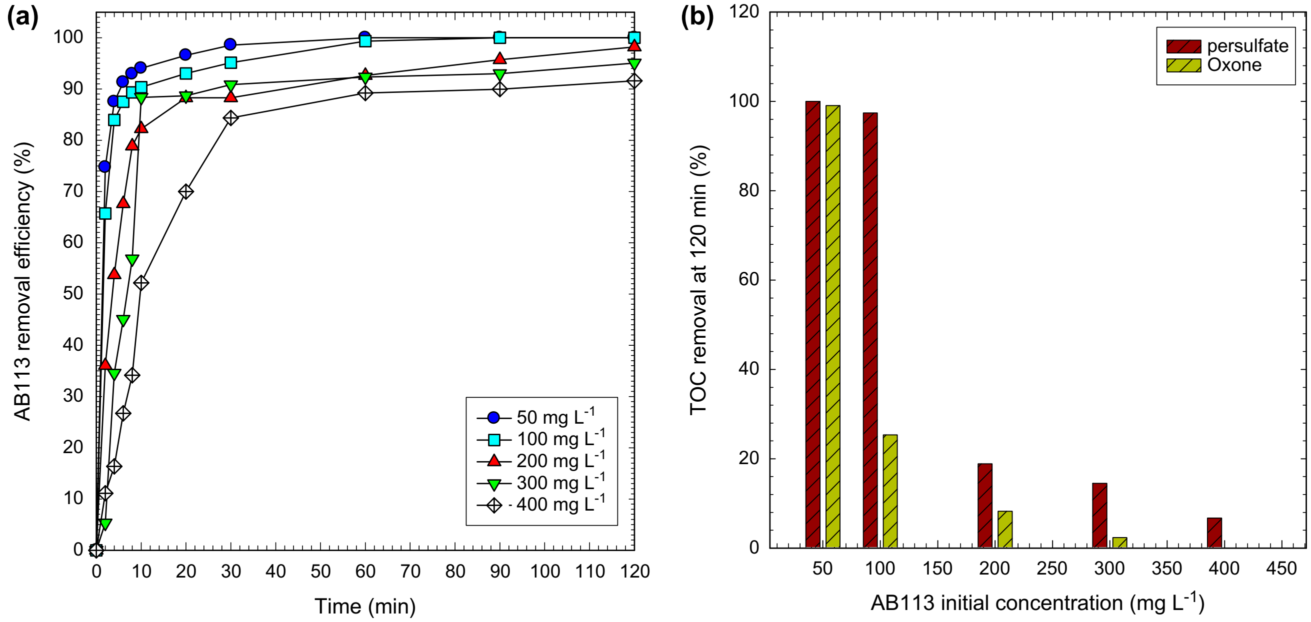

Fig. 7. Effect of initial AB113 concentration on (a) AB113 degradation by UV/PS and (b) TOC removal efficiencies by both UV/PS and UV/Oxone processes. The conditions were persulfate/Oxone dosage 6.3 mM, light intensity of 30 W $L^{-1}$, (5.6 mW $cm^{-2}$), and reaction time 120 min.

rate constants of UV/PS process are significantly higher than that of UV/Oxone process. And the second-order rate constant of UV/PS process is increasing with UV intensity exponentially. On the other hand, the second-order rate constant of UV/Oxone process is increasing smoothly and linearly with UV intensity.

As shown in Fig. 6(c), the mineralization of AB113 by UV/PS process is thorough when the highest persulfate dosage of 6.3 mM is applied for UV intensities from 2 to 5 mW cm$^{-2}$ that can reach 100% mineralization in 60–90 min. UV/Oxone process acts differently for AB113 mineralization. From Fig. 6(d), TOC removal efficiency increases proportionally to the UV intensity for reaction time of 60 min. For the lowest

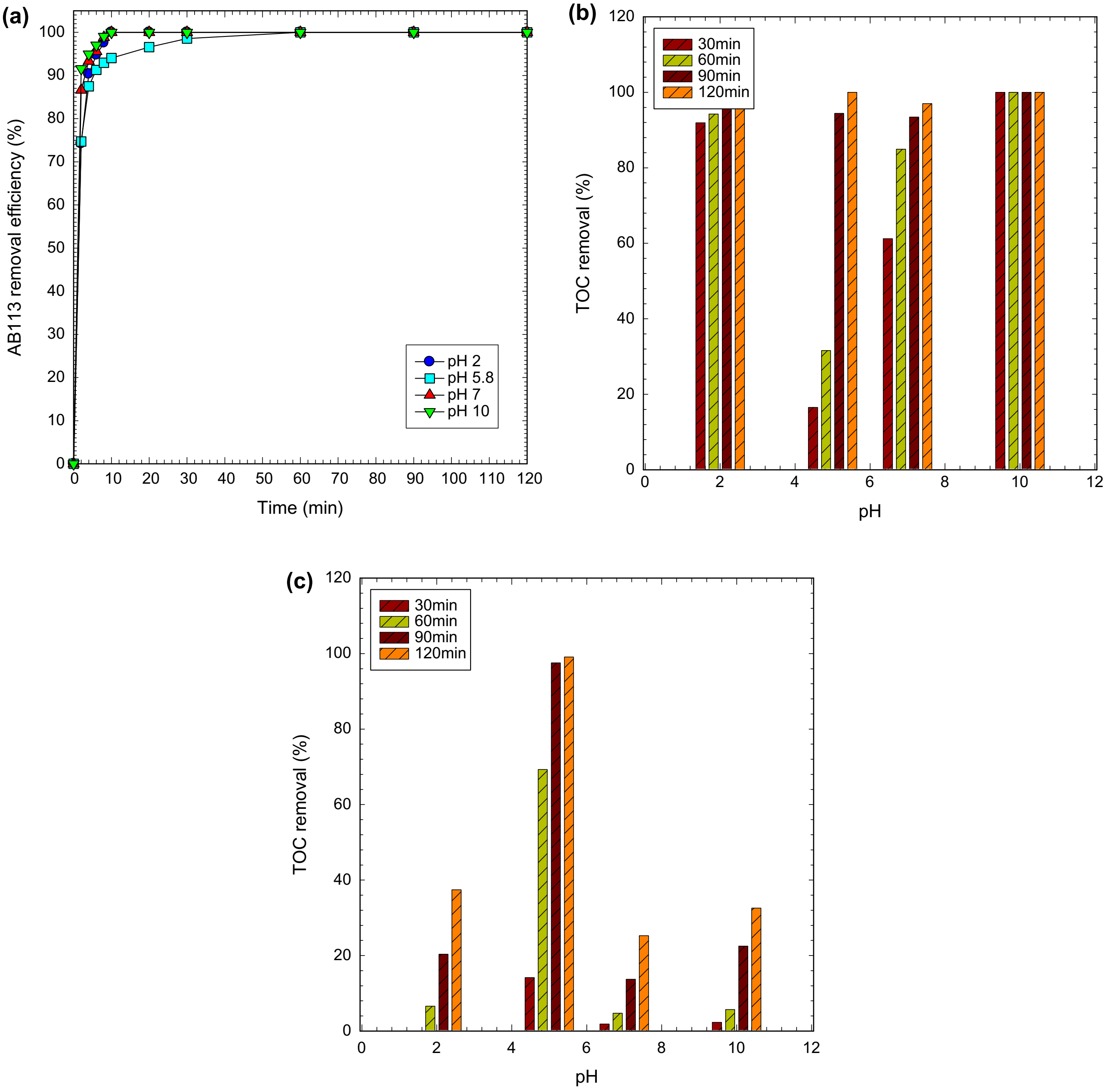

Fig. 8. Effect of pH on (a) AB113 removal by UV/PS process, (b) TOC removal by UV/PS process, and (c) TOC removal by UV/Oxone process. The conditions were initial dye concentration of 50 mg L$^{-1}$, persulfate/Oxone dosage of 6.3 mM, UV light intensity 30 W L$^{-1}$, (5.6 mW cm$^{-2}$), and reaction time during 120 min.

UV intensity of 2 mW $cm^{-2}$, the TOC removal efficiency is hardly changed.

There were very few researches presented the UV intensity effect on the decolorization of azo dye by UV/PS process according to the limitation of experimental setup. Salari et al. reported the treatment of basic yellow 2 by UV/PS process in an annular photoreactor with UV intensity of 5.5–40 W $m^{-1}$. They reported that the decolorization rate of dye increases with increasing light intensity which is consistent with this work [27].

### 3.5. Effect of initial dye concentration

To present the effect of initial AB113 concentration on the UV/PS process, it was studied at initial concentrations of 50–400 mg $L^{-1}$, persulfate dosage of 6.3 mM and 30 W $L^{-1}$ UV light intensity for a period of 120 min. Fig. 7(a) shows results of AB113 degradation as a function of reaction time at various initial AB113 concentrations. Results indicate that the second-order rate constant of AB113 removal decreases about 100 times from 0.028 to 0.0003 (L $mg^{-1}$ $min^{-1}$) when the initial dye concentration increases from 50 to 400 mg $L^{-1}$ as calculated from Fig. 7(a). Similar behavior of AB113 degradation by UV/Oxone process can be obtained as UV/PS process (data not shown). It is interested to find that the second-order rate constant, $k_2$, declines exponentially by raising initial dye concentration from 50 to 400 mg $L^{-1}$. The results are consistent to the observations by other researchers that the pseudo-first-order rate constant decreases with increasing of initial dye concentration [40]. As summarized in Fig. 7(b), the TOC removal efficiencies are 100, 97.4, and 18.8% in 120 min for initial AB113 concentration of 50, 100, and 200 mg $L^{-1}$, respectively for UV/PS process. Results indicated that the TOC removal was more sensitive to persulfate dosage than that of AB113 removal. The TOC removal efficiencies of UV/Oxone process are 99.1, 25.3, and 8.3% in 120 min for initial AB113 concentration of 50, 100, and 200 mg $L^{-1}$, respectively. It can be concluded that it is more difficult to mineralize AB113 at initial concentration higher than 100 mg $L^{-1}$ for UV/Oxone process.

### 3.6. Effect of pH

Fig. 8(a) shows AB113 degradation by UV/PS process as a function of time at various pH values. Results indicated that at original pH of 5.8, the AB113 removal efficiency reaches 94.0% in 10 min of UV/PS reaction. At pH 7, acidic pH of 2 and alkaline pH of 10, the AB113 degradation efficiencies all reach 100%. This implies that adjusting pH by either HCl or NaOH will provide beneficial effects on AB113 degradation by UV/PS process. However, the solution initial pH presents insignificant effect on AB113 degradation under UV/PS system as shown in Fig. 8(a). Similar AB113 degradation behavior is obtained for UV/Oxone process (data no shown).

Fig. 8(b) shows the TOC removal efficiency as a function of pH value for UV/PS process. Results indicate that at original pH 5.8, the TOC removal efficiencies are 16.5, 31.6, and 100% for reaction time of 30, 60, and 120 min, respectively for UV/PS process.

It is also worth to note that the TOC removal efficiencies can reach almost 100% in 120 min for all tested pH values. The pH value of 10 shows the best TOC mineralization with shortest reaction time. In contrast, pH 5 is the worst operating condition for TOC removal efficiency under UV/PS process. On the other hand, the original pH 5.8 shows the best TOC mineralization under UV/Oxone process. As shown in Fig. 8(c), the TOC removal efficiencies are 14.2, 69.3, and 99.1 for reaction time of 30, 60, and 120 min, respectively for UV/Oxone process. Under the pH values of 2, 7, and 10, UV/Oxone process can hardly mineralize TOC for less than 40% of removal efficiencies.

## 4. Conclusions

UV/PS and UV/Oxone processes were demonstrated to be promising treatment technologies for degradation and mineralization of AB113 wastewater. The oxidant (persulfate or Oxone) dosage was shown to be the most effective parameter to influence the AB113 and TOC removal rate among all operating parameters studied. For oxidant dosage from 0.21 to 6.3 mM, the higher the oxidant dosage applied, the higher the removal efficiency can be obtained. The optimal oxidant dosages are 2.1 and 4.2 mM for UV/PS and UV/Oxone processes, respectively. The second-order rate constant of AB113 removal increased with UV intensity increasing for both UV/PS and UV/Oxone processes. The initial pH was shown to be less effective on the AB113 degradation. However, pH value affects the TOC removal efficiency significantly for UV/Oxone process. The pH 5.8 is the best operating condition for TOC removal under UV/Oxone process. Overall, the UV/PS process demonstrates the better AB113 removal and TOC mineralization than UV/Oxone process.

## Acknowledgments

The authors appreciate the research funding granted by the Taiwan Ministry of Science and Technology (MOST 101-2221-E-241-004-MY3).

## References

[1] C.M. Kao, M.S. Chou, W.L. Fang, B.W. Liu, B.R. Huang, Regulating colored textile wastewater by 3/31 wavelength admi methods in Taiwan, Chemosphere 44 (2001) 1055–1063.

[2] M.C. Chang, C.P. Huang, H.Y. Shu, Y.C. Chang, A new photocatalytic system using steel mesh and cold cathode fluorescent light for the decolorization of azo dye orange G, Int. J. Photoenergy 2012 (2012) 303961.

[3] N.H. Ince, G. Tezcanlí, Reactive dyestuff degradation by combined sonolysis and ozonation, Dyes Pigm. 49 (2001) 145–153.

[4] A. Aris, P.N. Sharratt, Fenton oxidation of reactive black 5: Effect of mixing intensity and reagent addition strategy, Environ. Technol. 25 (2004) 601–612.

[5] I. Grčić, S. Papić, D. Mesec, N. Koprivanac, D. Vujević, The kinetics and efficiency of UV assisted advanced oxidation of various types of commercial organic dyes in water, J. Photochem. Photobiol. A: Chem. 273 (2014) 49–58.

[6] H.Y. Shu, M.C. Chang, Decolorization and mineralization of a phthalocyanine dye C.I. Direct Blue 199 using UV/$H_2O_2$ process, J. Hazard. Mater. 125 (2005) 96–101.

[7] C.R. Huang, H.Y. Shu, The reaction kinetics, decomposition pathways and intermediate formations of phenol in ozonation, UV/$O_3$ and UV/$H_2O_2$ processes, J. Hazard. Mater. 41 (1995) 47–64.

[8] H.Y. Shu, C.R. Huang, Decolorization of mono-azo dyes in wastewater by advanced oxidation process: A case study of acid red 1 and acid yellow 23, Chemosphere 29 (1994) 2597–2607.

[9] H.Y. Shu, M.C. Chang, H.J. Fan, Decolorization of azo dye acid black 1 by the UV/$H_2O_2$ process and optimization of operating parameters, J. Hazard. Mater. 113 (2004) 201–208.

[10] H.Y. Shu, W.P. Hsieh, Treatment of dye manufacturing plant effluent using an annular UV/$H_2O_2$ reactor with multi-UV lamps, Sep. Purif. Technol. 51 (2006) 379–386.

[11] M.S. Lucas, J.A. Peres, Decolorization of the azo dye Reactive Black 5 by Fenton and photo-Fenton oxidation, Dyes Pigm. 71 (2006) 236–244.

[12] M.C. Chang, H.Y. Shu, T.H. Tseng, H.W. Hsu, Supported zinc oxide photocatalyst for decolorization and mineralization of orange G dye wastewater under UV365 irradiation, Int. J. Photoenergy 2013 (2013) 595031.

[13] M.A. Dahmani, K. Huang, G.E. Hoag, Sodium persulfate oxidation for the remediation of chlorinated solvents (USEPA superfund innovative technology evaluation program), Water Air Soil Pollut.: Focus 6 (2006) 127–141.

[14] S.E. Denmark, D.C. Forbes, D.S. Hays, J.S. DePue, R.G. Wilde, Catalytic epoxidation of alkenes with oxone, J. Org. Chem. 60 (1995) 1391–1407.

[15] P. Ceccherelli, M. Curini, F. Epifano, M.C. Marcotullio, O. Rosati, Oxone oxidation of selenides: A mild and efficient method for the preparation of selenones, J. Org. Chem. 60 (1995) 8412–8413.

[16] A. Ishii, Y.-N. Jin, H. Nagaya, M. Hoshino, J. Nakayama, Reaction of 1,3-dithietanes with $2KHSO_5·KHSO_4·K2SO_4$: Scope and limitation for the preparation of dithiirane derivatives, Tetrahedron Lett. 36 (1995) 1867–1870.

[17] V.C. Mora, J.A. Rosso, G. Carrillo Le Roux, D.O. Mártire, M.C. Gonzalez, Thermally activated peroxydisulfate in the presence of additives: A clean method for the degradation of pollutants, Chemosphere 75 (2009) 1405–1409.

[18] P. Wang, S. Yang, L. Shan, X. Yang, W. Zhang, X. Shao, R. Niu, Waste heat-activated persulfate degradation of dye wastewater, Int. Conf. Bioinformatics Biomed. Eng., iCBBE (2010) 5514986.

[19] Q. Yang, H. Choi, Y. Chen, D.D. Dionysiou, Heterogeneous activation of peroxymonosulfate by supported cobalt catalysts for the degradation of 2,4-dichlorophenol in water: The effect of support, cobalt precursor, and UV radiation, Appl. Catal. B: Environ. 77 (2008) 300–307.

[20] S. Yang, P. Wang, X. Yang, L. Shan, W. Zhang, X. Shao, R. Niu, Degradation efficiencies of azo dye Acid Orange 7 by the interaction of heat, UV and anions with common oxidants: Persulfate, peroxymonosulfate and hydrogen peroxide, J. Hazard. Mater. 179 (2010) 552–558.

[21] S.Y. Oh, S.G. Kang, P.C. Chiu, Degradation of 2,4-dinitrotoluene by persulfate activated with zero-valent iron, Sci. Total Environ. 408 (2010) 3464–3468.

[22] J. Sun, X. Li, J. Feng, X. Tian, Oxone/$Co^{2+}$ oxidation as an advanced oxidation process: Comparison with traditional Fenton oxidation for treatment of landfill leachate, Water Res. 43 (2009) 4363–4369.

[23] P. Wang, S. Yang, L. Shan, R. Niu, X. Shao, Involvements of chloride ion in decolorization of Acid Orange 7 by activated peroxydisulfate or peroxymonosulfate oxidation, J. Environ. Sci. 23 (2011) 1799–1807.

[24] M.L. Crimi, J. Taylor, Experimental evaluation of catalyzed hydrogen peroxide and sodium persulfate for destruction of BTEX contaminants, Soil Sediment Contam. 16 (2007) 29–45.

[25] C. Liang, C.J. Bruell, Thermally activated persulfate oxidation of trichloroethylene: Experimental investigation of reaction orders, Ind. Eng. Chem. Res. 47 (2008) 2912–2918.

[26] Y.F. Huang, Y.H. Huang, Identification of produced powerful radicals involved in the mineralization of bisphenol A using a novel UV-$Na_2S_2O_8$/$H_2O_2$-Fe(II, III) two-stage oxidation process, J. Hazard. Mater. 162 (2009) 1211–1216.

[27] D. Salari, A. Niaei, S. Aber, M.H. Rasoulifard, The photooxidative destruction of C.I. Basic Yellow 2 using UV/$S_2O_8^{2-}$ process in a rectangular continuous photoreactor, J. Hazard. Mater. 166 (2009) 61–66.

[28] A. Rezaee, M.T. Ghaneian, A. Khavanin, S.J. Hashemian, G.H. Moussavi, G.H. Ghanizadeh, E. Hajizadeh, Photochemical oxidation of Reactive blue 19 dye (RB19) in textile wastewater by UV/$K_2S_2O_8$ process, Iran. J. Environ. Health Sci. Eng. 5 (2008) 95–100.

[29] Y.R. Wang, W. Chu, Degradation of a xanthene dye by Fe(II)-mediated activation of Oxone process, J. Hazard. Mater. 186 (2011) 1455–1461.

[30] M.C. Yeber, L. Díaz, J. Fernández, Catalytic activity of the $SO_4^-$ radical for photodegradation of the azo dye Cibacron Brilliant Yellow 3 and 3,4-dichlorophenol: Optimization by application of response surface methodology, J. Photochem. Photobiol. A: Chem. 215 (2010) 90–95.

[31] S.S. Abu Amr, H.A. Aziz, M.N. Adlan, M.J.K. Bashir, Pretreatment of stabilized leachate using ozone/persulfate oxidation process, Chem. Eng. J. 221 (2013) 492–499.

[32] J. Deng, Y. Shao, N. Gao, S. Xia, C. Tan, S. Zhou, X. Hu, Degradation of the antiepileptic drug carbamazepine upon different UV-based advanced oxidation processes in water, Chem. Eng. J. 222 (2013) 150–158.

[33] J.A. Khan, X. He, N.S. Shah, H.M. Khan, E. Hapeshi, D. Fatta-Kassinos, D.D. Dionysiou, Kinetic and mechanism investigation on the photochemical degradation of atrazine with activated $H_2O_2$, $S_2O_8^{2-}$ and $HSO_5^-$, Chem. Eng. J. 252 (2014) 393–403.

[34] C. Luo, J. Ma, J. Jiang, Y. Liu, Y. Song, Y. Yang, Y. Guan, D. Wu, Simulation and comparative study on the oxidation kinetics of atrazine by UV/$H_2O_2$, UV/$HSO_5^-$ and UV/$S_2O_8^{2-}$, Water Res. 80 (2015) 99–108.

[35] C.C. Lin, L.T. Lee, Degradation of polyvinyl alcohol in aqueous solutions using UV/oxidant process, J. Ind. Eng. Chem. 21 (2015) 569–574.

[36] X. He, A.A. de la Cruz, K.E. O'Shea, D.D. Dionysiou, Kinetics and mechanisms of cylindrospermopsin destruction by sulfate radical-based advanced oxidation processes, Water Res. 63 (2014) 168–178.

[37] J. Sharma, I.M. Mishra, V. Kumar, Degradation and mineralization of Bisphenol A (BPA) in aqueous solution using advanced oxidation processes: UV/$H_2O_2$ and UV/$S_2O_8^{2-}$ oxidation systems, J. Environ. Manage. 156 (2015) 266–275.

[38] C. Tan, N. Gao, Y. Deng, Y. Zhang, M. Sui, J. Deng, S. Zhou, Degradation of antipyrine by UV, UV/$H_2O_2$ and UV/PS, J. Hazard. Mater. 260 (2013) 1008–1016.

[39] T. Olmez-Hanci, D. Dursun, E. Aydin, I. Arslan-Alaton, B. Girit, L. Mita, N. Diano, D.G. Mita, M. Guida, $S_2O_8^{2-}$/UV-C and $H_2O_2$/UV-C treatment of Bisphenol A: Assessment of toxicity, estrogenic activity, degradation products and results in real water, Chemosphere 119 (2015) 115–123.

[40] H.Y. Shu, M.C. Chang, H.J. Fan, Effects of gap size and UV dosage on decolorization of C.I. Acid Blue 113 wastewater in the UV/$H_2O_2$ process, J. Hazard. Mater. 118 (2005) 205–211.

[41] Y.O. Kim, H.U. Nam, Y.R. Park, J.H. Lee, T.J. Park, T.H. Lee, Fenton oxidation process control using oxidation-reduction potential measurement for pigment wastewater treatment, Korean J. Chem. Eng. 21 (2004) 801–805.

[42] H.Y. Shu, M.C. Chang, S.W. Huang, Decolorization and mineralization of azo dye Acid Blue 113 by the UV/Oxone process and optimization of operating parameters, Desalin. Water Treat. 57 (2015) 7951–7962.

[43] D. Kamel, A. Sihem, C. Halima, S. Tahar, Decolourization process of an azoïque dye (Congo red) by photochemical methods in homogeneous medium, Desalination 247 (2009) 412–422.